

DESIGN OF THE RECIRCULATING LINAC OPTION FOR THE UK NEW LIGHT SOURCE

P. H. Williams*, D. Angal-Kalinin, D. Dunning, J. K. Jones & N. R. Thompson,
STFC, Daresbury Laboratory, ASTeC & Cockcroft Institute, UK
R. Bartolini, I. P. Martin, & J. Rowland, Diamond Light Source Ltd. & John Adams Institute, UK

Abstract

We present progress in the design of the recirculating linac option for the UK New Light Source (NLS). Improvements in all accelerator sections have been made such that the output meets the required specifications to drive the seeded NLS free-electron lasers (FELs). Full start-to-end simulations are presented.

INTRODUCTION

The New Light Source project [1] has developed a science case and conceptual facility design for a next generation light source for the UK based on a suite of seeded free-electron lasers.

The progress on the NLS design is described in [2] and the beam dynamics optimisation for the single pass linac is described in [3]. The science case requires repetition rates of up to 1 MHz, therefore NLS is based on a superconducting linac. Superconducting infrastructure necessitates comparatively large capital outlay and running costs, these can be mitigated by recirculating in a linac of lower energy. It is therefore important to investigate whether it is possible to design a recirculating linac capable of delivering the challenging bunch parameters viz; a 200 pC bunch with small emittances and energy spread with peak current of more than 1 kA to drive the FELs. The seeded nature also demands that bunch slice parameters remain constant over 100 fs.

In addition to the beam dynamics limitations one must consider for a single pass linac, recirculation entails demanding optics designs of mergers, separators, arcs and additional transport. The bunch compression scheme becomes restricted due to the topology and coherent synchrotron radiation in bending sections.

The NLS recirculating linac has undergone significant modification and optimisation from that presented at [4]. The resulting simulated bunch has been passed through FEL simulations to demonstrate the capability of the recirculating linac.

FACILITY DESIGN

Fig. 1 shows a schematic layout of the NLS recirculating linac. The design philosophy is to minimise any bunch compression from components not dedicated for that purpose, in other words separating as much as possible trans-

verse and longitudinal manipulations. In this way, one retains the ability to tailor the final bunch profile in a flexible way.

The gun is followed by two cryomodules, the first of whose cavities are fed from individual power supplies to enable independent phase and voltage control for emittance compensation in the gun. Tracking using Elegant [5] commences at this location. The beam is decelerated and linearised in longitudinal phase space using a third harmonic (3.9 GHz) system capable of achieving 16 MV/m in CW operating mode. The particular gradient required to linearise the bunch is a function not only of the accelerating RF, but also of the T_{566} in subsequent components. This is followed by the first four-dipole C-type compressor chicane. The beam then enters an isochronous and achromatic injection dogleg. This uses two dipoles in addition to the last dipole of a standard four dipole chicane, which is that traversed by the high energy beam.

On first pass through the seven cryomodules of the main linac, the beam energy is raised to 1.2 GeV. The beam passes through an extraction dipole which deflects this beam by 10° and allows separation from the higher energy recirculated beam. Five quadrupoles are followed by a -10° dipole, thus forming an achromatic dogleg, then four additional quadrupoles match to the arc.

The arcs are based on the BESSY-FEL design [6]. Each 180° arc consists of four triple-bend achromats ($\pi/12$ dipole bend angle) and was chosen due to the small incoherent synchrotron radiation (ISR) induced emittance dilution of the beam (4% total for both arcs). Coherent synchrotron radiation (CSR) does not degrade the beam significantly if the bunch length is kept above 2 ps FW through the arcs.

Exiting the second arc, the beam enters an exact reverse of the linac-to-arc matching. This is followed by the second four-dipole compressor chicane, which is of S-type in order to reduce emittance growth due to CSR. It then traverses the high-energy branch of the injection system and passes through the linac a second time, reaching an energy of 2.2 GeV.

The extraction system consists of three dipoles in addi-

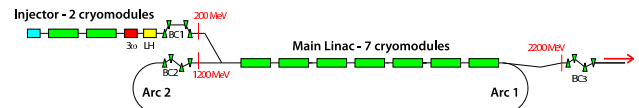


Figure 1: Layout of the NLS recirculating linac.

*peter.williams@stfc.ac.uk

tion to the extraction dipole and ten quadrupoles. The final four-dipole compression chicane is of S-type to minimise CSR emittance growth.

The beam then passes through a collimation section and spreader system to the FELs, this is identical to the single pass machine and is described in [7].

OPTIMISATIONS

Because of the large energy spreads required for bunch compression, it is important that all sections of the recirculating linac are well behaved at second order in the transfer matrices. To achieve this, a brute force method of chromatic and geometric aberration correction has been employed. We use a Nelder-Mead simplex optimisation to minimise the horizontal and vertical emittances and T_{566} using the number, strengths and positions of sextupoles as the optimisation variables in relevant sections. This has been performed for the injection achromat, linac-to-arc and arc-to-linac matching sections. With an energy spread of $\mathcal{O}(3\%)$, the injection achromat requires the strongest correction of these and the results of the optimisation are shown in Fig. 2 as an example of the technique. The op-

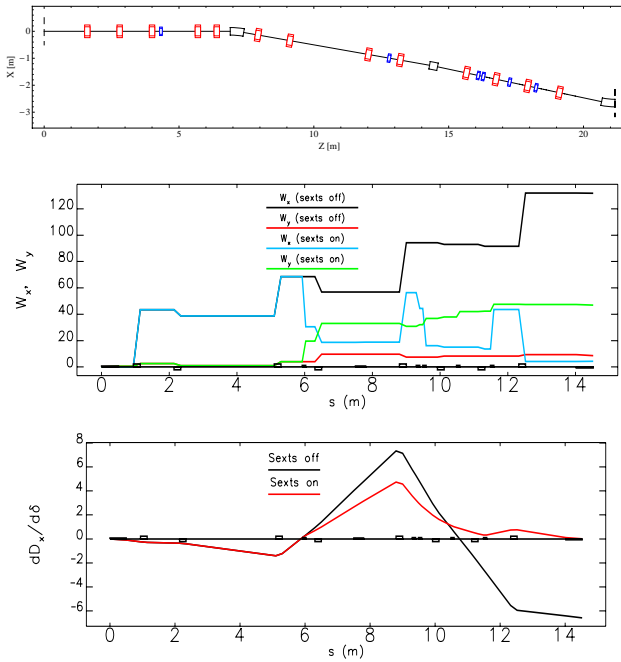


Figure 2: Injection achromat: (1) layout, sextupoles in blue, (2) chromatic amplitude functions before (black, red) and after (blue, green) correction, (3) chromatic derivative of dispersion before (black) and after (red) correction

timisation settled on a system of six sextupoles, five in the dispersive section and one in the preceding matching section to control the geometric second order terms. Fig. 2 shows that the chromatic amplitude functions are reduced by a factor of ten in the horizontal plane although at the cost of a slight increase in the vertical plane. Also shown is that the chromatic derivative of dispersion is fully cor-

rected. The value of T_{566} before correction is -1.13 and after is -0.35 , a fourfold reduction. This reduces the gradient required in the third harmonic cavity.

After the second pass through the linac, the 2.2 GeV beam is deflected 5.5° by the extraction dipole. CSR driven emittance increase from this dipole is of concern because the bunch has become short by this point. Indeed, failure to address this has been shown to increase the emittance by an order of magnitude. To mitigate this, the horizontal beta function must be minimised at the dipole. This is a non-trivial task as the quadrupoles in the linac also focus the first pass beam, and with higher k-values. Therefore we perform a dual optimisation of the optics in the linac at 1.2 GeV and 2.2 GeV simultaneously and subsequently match both the linac-to-arc matching and the extraction system. The results of this optimisation are shown in Fig. 3.

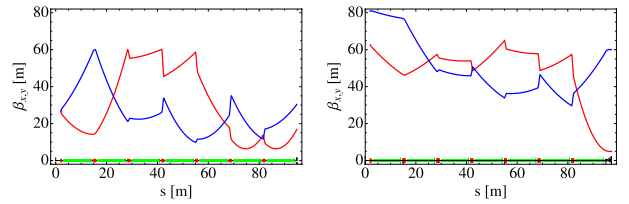


Figure 3: Optimised optics through the linac at (1) 1.2 GeV and (2) 2.2 GeV simultaneously (red - horizontal, blue - vertical).

Optimisation of the longitudinal phase space (progressive bunch compression) through the machine is predominantly governed by the strengths of the three bunch compressors, the off crest chirp imparted in the injector, first and second passes of the main linac, and the gradient and phase of the third harmonic cavity. The highly non-linear nature of this eight dimensional optimisation problem forces us to abandon the Nelder-Mead simplex method which becomes stuck at a local minimum in the penalty function. Instead, we adopt the Luus-Jaakola pseudo-random global minimum search algorithm [8].

FINAL BUNCH PROPERTIES

Table 1 shows the machine parameters optimised to produce the final bunch. Fig. 4 shows that despite all transport we only increase the horizontal projected emittance from 0.3 to 0.6 mm mrad. Fig. 5 shows the final slice properties.

FEL RESULTS

Time dependent FEL simulations [9] have been carried out for FEL-3 operating at 1 keV photon energy. The bunching and energy spread values at the centre of the seeded region were found to agree well with steady-state results. The variation of peak radiation power at the fundamental with distance through the radiator is shown in

Table 1: Optimised machine parameters. Phases are with respect to crest.

Optimised Section	Variable	Value
3 ω lineariser	E	16 MV/m
3 ω lineariser	ϕ	+160.9°
Injector	ϕ	-29.1°
Linac first pass	ϕ	-11.8°
Linac second pass	ϕ	+2.3°
Bunch compressor 1	R_{56}	-96.7 mm
Bunch compressor 2	R_{56}	-80.9 mm
Bunch compressor 3	R_{56}	-23.9 mm

Table 2: Bunch length and energy spread at salient points.

Section	Energy	σ_z (FW)	σ_δ (FW)
Start of tracking	136 MeV	18 ps	2.8 %
After BC1	228 MeV	5 ps	3.5 %
Matching to arc 1	1227 MeV	6 ps	1.5 %
After BC2	1227 MeV	900 fs	1.5 %
After BC3	2244 MeV	350 fs	0.6 %

Fig. 6, compared to the equivalent result using the single pass bunch of [3]. Also shown is the variation of the radiation bandwidth with distance through the radiator; the seeded part of the bunch is considered to have reached saturation when this is minimised. For the recirculator, the seeded part of the bunch reaches saturation at 20 m, at which point the output power is 1 GW. The power continues to increase beyond this point, but the temporal radiation profile quality becomes degraded. Also shown is a comparison of the evolution of the temporal radiation profile with distance through the radiator.

CONCLUSIONS

We have presented a complete start-to-end design for the NLS using a recirculating linac. This design needed many novel design concepts as well as optimisation procedures to achieve the challenging bunch parameters needed to drive seeded FELs. We have produced a bunch satisfying most requirements and passed it through FEL simulations to demonstrate that it is possible to use such a design.

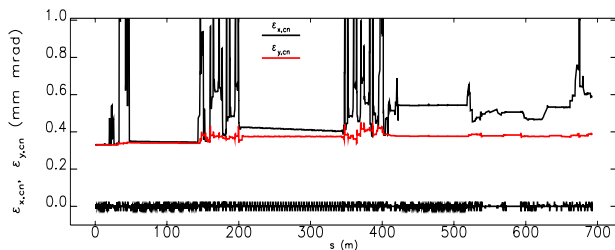


Figure 4: Projected normalised emittances from gun to FEL.

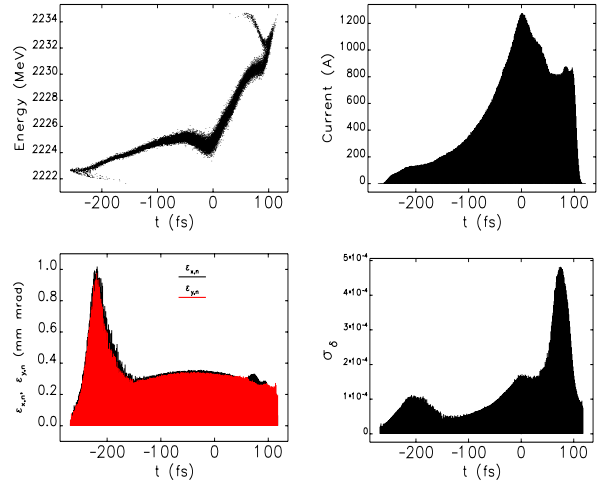


Figure 5: Final bunch properties: (1) longitudinal phase space, (2) current profile, (3) slice emittances & (4) slice energy spread.

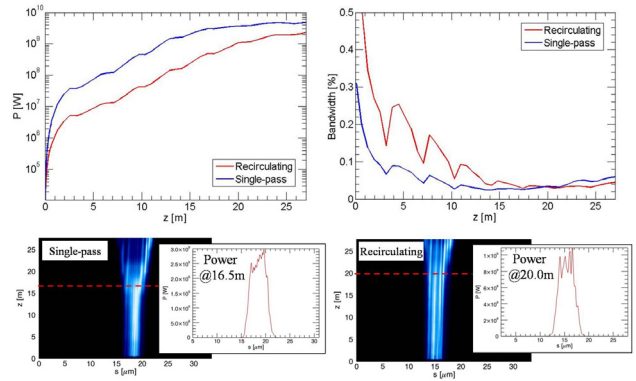


Figure 6: A comparison of time-dependent FEL simulations at 1 keV photon energy for the NLS recirculating and single pass linacs: (1) peak radiation power with distance through radiator, (2) radiation bandwidth with distance through radiator, (3) & (4) evolution of temporal radiation profile with distance through radiator.

REFERENCES

- [1] J. Marangos *et al.*, NLS Project: Conceptual Design Report, <http://www.newlightsource.org>.
- [2] R. Walker *et al.*, TUPE055, these proceedings.
- [3] R. Bartolini *et al.*, WEPEA065, these proceedings.
- [4] P. H. Williams *et al.*, 31st International Free-Electron Laser Conference, Liverpool, August 2009.
- [5] M. Borland, Advanced Photon Source, LS-287 (2000).
- [6] M. Abo-Bakr *et al.*, BESSY-FEL Technical Design, 2004.
- [7] D. Angal-Kalinin *et al.*, TUPEC036, these proceedings.
- [8] R. Luus & T. H. I. Jaakola, AICHE Journal **19**, 760 (1973).
- [9] S. Reiche, Nucl. Instrum. Methods in Phys. Res. **A429**, 243 (1999).